Electromagnetically induced transparency without a Doppler background in a multilevel ladder-type cesium atomic system

Baodong Yang,[1,2] Jing Gao,[1] Tiancai Zhang,[1] and Junmin Wang[1,*]

[1]*State Key Laboratory of Quantum Optics and Quantum Optics Devices, and Institute of Opto-Electronics, Shanxi University, Taiyuan 030006, P. R. China*

[2]*College of Physics and Electronic Engineering, Shanxi University, Taiyuan 030006, P. R. China*

(Received 29 September 2010; published 21 January 2011)

We present an investigation of electromagnetically induced transparency (EIT) without Doppler background due to a locked probe laser. The EIT is theoretically studied based on a multilevel ladder-type cesium atomic system $6S_{1/2}$–$6P_{3/2}$–$8S_{1/2}$ in a room-temperature vapor cell. The experimental results agree with the theoretical calculations. Compared with the traditional EIT spectra with a Doppler profile limiting the spectral resolution for keeping the coupling laser locked and scanning the probe laser, these EIT spectra with the probe laser locked and the coupling laser scanned have a flat background, which seem be of great benefit for applications such as the measurement of hyperfine intervals between excited states, the study of highly excited Rydberg states, laser-frequency stabilization, etc.

DOI: 10.1103/PhysRevA.83.013818 PACS number(s): 42.50.Gy, 42.62.Fi, 32.80.Qk, 32.80.Xx

I. INTRODUCTION

Electromagnetically induced transparency (EIT) is a quantum destructive interference effect that allows propagation of a weak probe laser through an opaque atomic medium when a strong coupling laser is present. It was theoretically proposed in 1989 [1] and proven experimentally in 1991 [2]. Since then, the EIT effect has attracted considerable attention because of its potential applications in many fields such as quantum memory [3], quantum repeater [4], quantum metrology [5], Rydberg atomic-state detection [6], laser-frequency stabilization [7], etc.

Many studies of EIT are based on an ideal three-level model in Λ, V, or ladder types [8–10]. However, atoms often have complicated energy-level structures instead of following an ideal model. Furthermore, conventional EIT spectra are often obtained by scanning the probe laser while keeping the coupling laser resonant with the transition or at a certain frequency detuning, so the EIT signals unavoidably have a Doppler background that limits the spectral resolution of the EIT in a vapor cell at room temperature [11]. In our experimental scheme, EIT spectra without a Doppler background are observed by scanning the frequency of the coupling laser while locking the frequency of the probe laser in a room-temperature cesium vapor cell.

Our observations are in accordance with our theoretical calculations, which are based upon a multilevel ladder-type model. This technique uses EIT to transfer information about a weak transition between excited states to a strong probe transition, and its spectra usually have a narrow line width due to atomic coherence effects, and it is applicable to excited-state transitions allowing, in principle, a large number of additional potential optical frequency references [7]. We also believe that the EIT spectra without a Doppler background should be more beneficial for precise determination of the hyperfine splitting of excited states and the hyperfine structure constant, direct optical detection of highly excited Rydberg states, etc.

*Author to whom correspondence should be addressed, email: wwjjmm@sxu.edu.cn

II. EXPERIMENTAL SETUP

Figure 1 shows the relevant hyperfine levels $6S_{1/2}$–$6P_{3/2}$–$8S_{1/2}$ of a cesium atom. The spontaneous decay rate for the $6P_{3/2}$–$6S_{1/2}$ transition is $\Gamma_{21}/(2\pi) = 5.22$ MHz, and that for the $8S_{1/2}$–$6P_{3/2}$ transition is $\Gamma_{32}/(2\pi) = 2.18$ MHz. The $6S_{1/2}$–$6P_{3/2}$ transition is coupled by the probe laser with Rabi frequency Ω_p and detuning Δ_p, while the $6P_{3/2}$–$8S_{1/2}$ transition is driven by the coupling laser with Rabi frequency Ω_c and detuning Δ_c.

A schematic of experimental setup is shown in Fig. 2. A commercial grating-feedback external-cavity diode laser (ECDL) at 794.6 nm (Toptica DL-100 L) with typical line width of ~500 KHz (in 50 ms) serves as the coupling laser scanning over the $6P_{3/2}$–$8S_{1/2}$ transition, while a home-made ECDL at 852.3 nm with roughly the same line width is used as the probe laser. The latter can be locked to one of the $6S_{1/2}$–$6P_{3/2}$ hyperfine transitions by the conventional frequency-modulation technique combined with saturated-absorption spectroscopy. In our experiment, the coupling and probe lasers were in the counterpropagating (CTP) configuration to eliminate the Doppler effect when $\omega_p \sim \omega_c$ [12,13]. The two laser beams with a diameter ~2.0 mm for the probe beam and ~2.2 mm for the coupling beam overlapped in the cesium vapor cell (diameter: 25 mm, length: 50 mm) with dichroic filters (DFs), and then the probe beam was separated to the photodiode (PD) by DF2. The EIT spectra without a Doppler background from the PD are recorded on a digital storage oscilloscope (not shown in Fig. 2), and the frequency interval is calibrated using a confocal Fabry-Perot cavity (not shown in Fig. 2) with a finesse of 100 and a free spectral range (FSR) of 735 MHz.

III. EXPERIMENTAL RESULTS AND THEORETICAL DISCUSSIONS

A. Experimental results of EIT spectra without Doppler background

In order to obtain the EIT spectra without a Doppler background, we lock the probe laser to the $6S_{1/2}F = 3$–$6P_{3/2}F' = 2$ hyperfine transition and scan the coupling laser

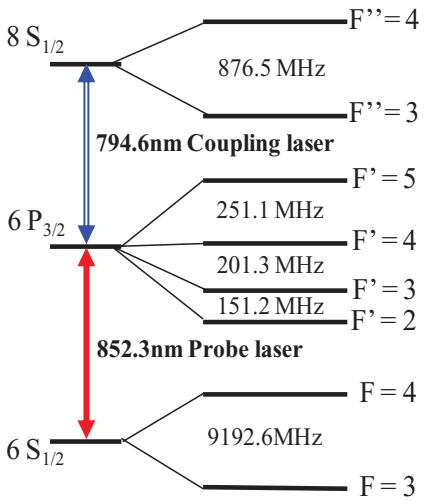

FIG. 1. (Color online) Relevant energy levels of cesium atoms.

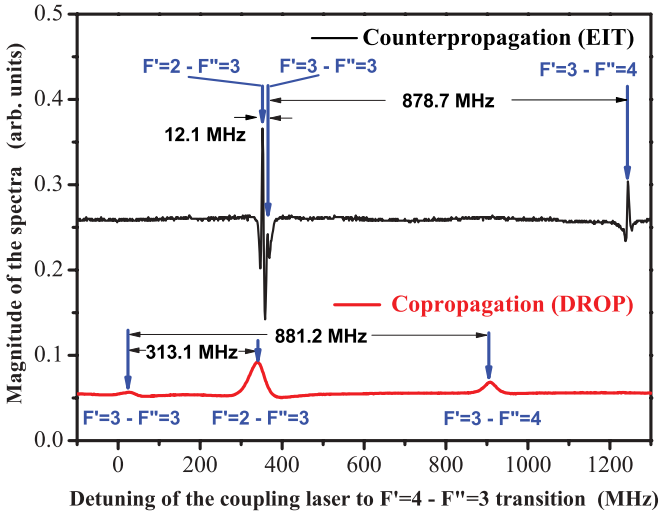

FIG. 3. (Color online) EIT spectra without Doppler background for counterpropagating (CTP) configuration and DROP spectra for copropagating (CP) configuration when the probe laser is locked to the $6S_{1/2}F = 3$–$6P_{3/2}F' = 2$ transition and the coupling laser is scanned over the $6P_{3/2}$–$8S_{1/2}$ transition.

across the $6P_{3/2}$–$8S_{1/2}$ transition, which is contrary to the scanning mode used for traditional EIT spectroscopy with a Doppler background. In addition, we note that there exists simultaneously two kinds of optical-pumping effects: one is single-resonance optical pumping (SROP), which is based on population transferring from one of the ground-state hyperfine components to another via spontaneous decay through one of intermediate states [14], and the other is double-resonance optical pumping (DROP), which is based on population transferring from one of the hyperfine folds of the ground state to another via the two-photon excitation process to higher excited states and spontaneous decay through the intermediate states in a ladder-type atomic system [15,16]. These two kinds of optical-pumping effects make the probe laser more transparent for decreasing populations on the $F = 3$ hyperfine fold of $6S_{1/2}$ ground state; they are always mixed into EIT spectra. In our scheme, the probe laser is locked onto the $6S_{1/2}F = 3$–$6P_{3/2}F' = 2$ cycle transition to avoid the SROP effect, and the probe laser power is set to ~88 μW [$\Omega_p/(2\pi) =$ 4.78 MHz $< \Gamma_{21}/(2\pi) = 5.22$ MHz] to reduce the population of the $6P_{3/2}F' = 2$ intermediate state, therefore decreasing the DROP effect. Figure 3 shows the EIT spectra for the CTP configuration; here the coupling laser power is ~8 mW. In order to compare the line width, we also show DROP spectra for the copropagating (CP) configuration in Fig. 3.

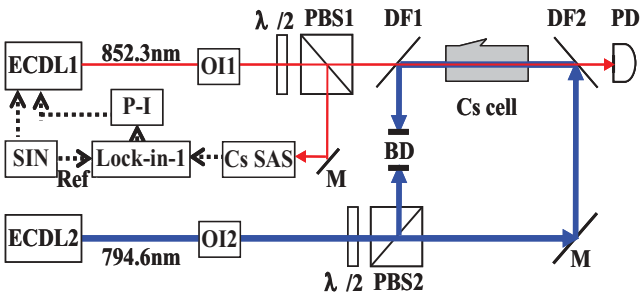

FIG. 2. (Color online) Schematic of experimental setup. Keys to figure: ECDLs: external cavity diode lasers; SIN: sine-wave signal generator; Lock-in: lock-in amplifier; OI: optical isolator; PD: photodiode; P-I: proportion and integration amplifier; λ/2: half-wave plate; PBS: polarization beam splitter cube; SAS: saturated absorption spectroscopy; Ref: reference channel of lock-in amplifier; DF, dichroic filter; BD, beam dump.

For the DROP spectra, the peaks from left to right correspond to the transitions between the levels $6P_{3/2}F' = 3$–$8S_{1/2}F'' = 3$, $6P_{3/2}F' = 2$–$8S_{1/2}F'' = 3$, and $6P_{3/2}F' = 3$–$8S_{1/2}F'' = 4$; their positions are on a two-photon resonance ($\Delta_p + \Delta_c \sim 0$) and their magnitudes are dependent on the DROP rate [17]. The peak corresponding to the $6P_{3/2}F' = 2$–$8S_{1/2}F'' = 3$ transition results from the contribution of approximately-zero-velocity atoms in the $6S_{1/2}F = 3$ ground state in the direction of the laser beam because the probe laser is locked to the $6S_{1/2}F = 3$–$6P_{3/2}F' = 2$ transition. The other two peaks are due to the contributions of some atoms with velocities of ~128.8 m/s (the Doppler frequency shift $\Delta\upsilon = \upsilon\upsilon_0/c = 151.2$ MHz, in which υ is the velocity of atoms in the direction of the probe beam, υ_0 is the probe laser frequency, c is the speed of light, and 151.2 MHz is the frequency interval between the $6P_{3/2}F' = 2$ and $6P_{3/2}F' = 3$ states) with a frequency detuning of 151.2 MHz from the probe laser, and these atoms have a frequency detuning of 151.2 × (852.3/794.6) = 162.2 MHz from the coupling laser. So the frequency interval of the two remaining peaks is 151.2 + 162.2 = 313.4 MHz, which is consistent with the experimental value of 313.1 MHz, as shown in Fig. 3. In addition, the frequency interval of the peaks on both sides is ~881.2 MHz in the experiment, which is comparable to 876.5 MHz, as indicated in Fig. 1. The difference between them may be due to the nonlinear scanning of the coupling laser's piezo in the external cavity and the errors from the determination of the center of the related DROP peaks whose line width is broader compared with the EIT spectra.

The EIT spectra in Fig. 3 contain three lines corresponding to the resonant transition between $6S_{1/2}F = 3$–$6P_{3/2}F' = 2$–$8S_{1/2}F'' = 3$ and the detuned transitions at -151.2 MHz with respect to the probe laser between $6S_{1/2}F = 3$–$6P_{3/2}F' = 3$–$8S_{1/2}F'' = 3$, 4, as indicated by arrows from left to right, respectively. Similar experimental results have been reported in Ref. [18] but were obtained by scanning the probe laser while keeping the coupling laser on-resonance; therefore, their spectra often have a Doppler background. Compared with the above DROP spectra, accompanied by spontaneous decay for the CP configuration, the EIT spectra, which is based on atomic coherence for the CTP configuration, has a higher signal-to-noise (SN) ratio and a narrower line width, as shown in Fig. 3, so it is obviously more suitable for the precise measurement of the hyperfine splitting and the hyperfine structure constant. In this CTP configuration, although DROP exists (which also makes the probe laser transparent) and its scanning mode [17] is the same as for the EIT spectra without a Doppler background, it cannot perfectly interpret the spectral profile, especially for some additional absorption dips on both sides of the transparent peaks, as show in Fig. 3. It also contributes only a little to the spectra for a weak probe laser, which lowers the population in intermediate states. Furthermore, EIT makes the probe beam more transparent, and so also suppresses the DROP to a certain degree. The following EIT theory, which is based on a multilevel model, gives a reasonable explanation for the spectra of the CTP configuration.

B. Theoretical analysis based on a multilevel ladder-type model

In this section, we compare our experimental results with a theoretical treatment. EIT has been well studied theoretically and experimentally, and it is substantially interpreted that the atoms are prepared in a dark superposition state. However, just recently, EIT spectra without a Doppler background have been reported in a new scanning mode [6,16]. In addition, the essential physics of EIT have been well understood based on investigations of the ideal three-level model; in fact, the atom often has a complicated multilevel structure which gives rise to several interesting features: (1) It is possible to create multiple EIT windows simultaneously supporting slow group velocities for two or more probe pulses at different frequencies in such systems [19]. (2) Multilevel EIT systems may be useful for nonlinear generation processes [20]. In the complex susceptibility $\chi = \chi' + i\chi''$, the real part χ' and imaginary part χ'' are related to the dispersion and absorption of the atomic medium, respectively [12]:

$$\chi(v)\,dv = \frac{4i\hbar g_{21}^2/\varepsilon_0}{\gamma_{21} - i\Delta_p - i\frac{\omega_p}{c}v + \frac{\Omega_c^2/4}{\gamma_{31} - i(\Delta_p + \Delta_c) - i(\omega_p \pm \omega_c)v/c}} N(v)\,dv, \tag{1}$$

$$N(v) = \frac{N}{u\sqrt{\pi}} e^{-v^2/u^2} dv, \tag{2}$$

$$u = \sqrt{\frac{2kT}{m}}. \tag{3}$$

In Eq. (1), the plus sign is used for the CP configuration and the minus sign for the CTP configuration and $\Omega_p = 2g_{21}E_p$, where g_{21} is the dipole moment matrix element for the $6S_{1/2}$–$6P_{3/2}$ hyperfine transitions and E_p is the amplitude of the probe laser. The quantity $N(v)$ is the one-dimensional Maxwell-Boltzmann velocity distribution, and u is the most probable velocity. The Boltzmann constant is k, T is temperature, and m is the mass of a cesium atom. Equation (1) gives the EIT signal for the CTP configuration in a room-temperature atomic vapor cell for a ladder-type system, because the small term $(\omega_p - \omega_c)v/c$ can be neglected because $\omega_p \sim \omega_c$. However, the EIT signal is nearly submerged by the Doppler effect because the term $(\omega_p + \omega_c)v/c$ cannot be ignored for the CP configuration [12].

Here, the system $6S_{1/2}F = 3$–$6P_{3/2}F' = 2$–$8S_{1/2}F'' = 3$ is regarded as the resonant EIT signal in which the probe laser is locked onto the $6S_{1/2}F = 3$–$6P_{3/2}F' = 2$ hyperfine transition while the coupling laser is scanned across the $6P_{3/2}$–$8S_{1/2}$ transition. At the same time, the $6S_{1/2}F = 3$–$6P_{3/2}F' = 3$–$8S_{1/2}F'' = 3(4)$ system will be the detuning -151.2-MHz EIT signal with respect to the $6S_{1/2}F = 3$–$6P_{3/2}F' = 2$ transition because some atoms with velocities of $\sim$128.8 m/s will be populated on the $6P_{3/2}F' = 3$ state in this scanning mode. The $6P_{3/2}F' = 4$ hyperfine state will have little contribution to the signal for the large frequency detuning of -352.5 MHz, as shown in Fig. 1, so we do not include it in the calculation. Furthermore, we know the Rabi frequencies corresponding to different transitions are different. Here, the Rabi frequency Ω_c of the coupling laser between intermediate states and higher excited states is not crucial, because it would affect the magnitudes of EIT peaks rather than their positions. Thus, Ω_c is a free parameter in the calculation. For probe laser, we let $\Omega_{32} = a_{32}\Omega_p$ (Ω_{32} is the Rabi frequency of the transition $F = 3$–$F' = 2$), and $\Omega_{33} = a_{33}\Omega_p$ (Ω_{33} corresponds to the transition F = 3–$F' = 3$), where the relative strength of two transitions a_{32}:$a_{33} \approx 1$:1.05 [21].

Finally, the superposition of the above two partial signals (resonance and detuning -151.2 MHz) calculated from the imaginary χ'' according to the relative strength a_{32}:a_{33} is shown in Fig. 4 and is very similar to the experimental result shown in Fig. 3. The frequency interval between the two left peaks in Fig. 4 is 11.0 MHz, which is comparable with the experimental value of 12.1 MHz in Fig. 3. The frequency interval between the two right peaks should be 876.5 MHz, and the experimentally measured value is 878.7 MHz. The main discrepancy is due to the nonlinear effect of the coupling laser's piezo in the external cavity. An alternative and more precise method, in which we use the frequency interval between the carrier and the modulation sideband of a radio-frequency phase-modulated laser beam injected into the confocal Fabry-Perot cavity as a frequency calibrator, will be employed in a future experiment.

On the other hand, some additional absorption dips on both sides of the transparent signals in Fig. 3 result from a wavelength mismatch between probe and coupling lasers, which are confirmed by calculation as shown in Fig. 4. According to Eq. (1), when not considering the Doppler

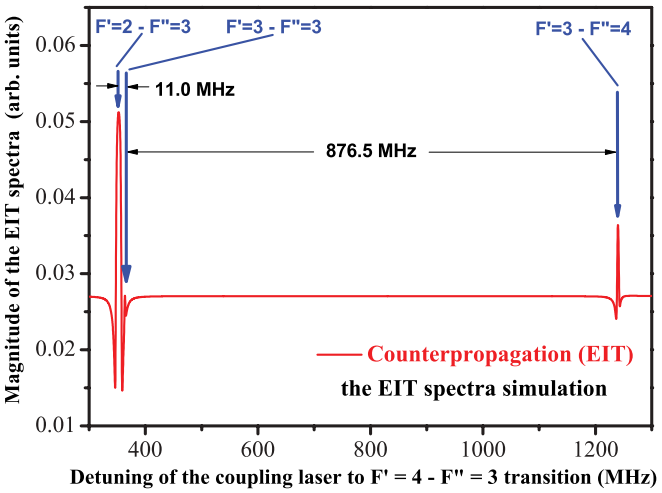

FIG. 4. (Color online) Simulation for EIT spectra without Doppler background. Simulation is based on a multilevel ladder-type model for counterpropagating (CTP) configuration when the probe laser is locked to the $6S_{1/2}F = 3$–$6P_{3/2}F' = 2$ transition and the coupling laser is scanned over the $6P_{3/2}$–$8S_{1/2}$ transition.

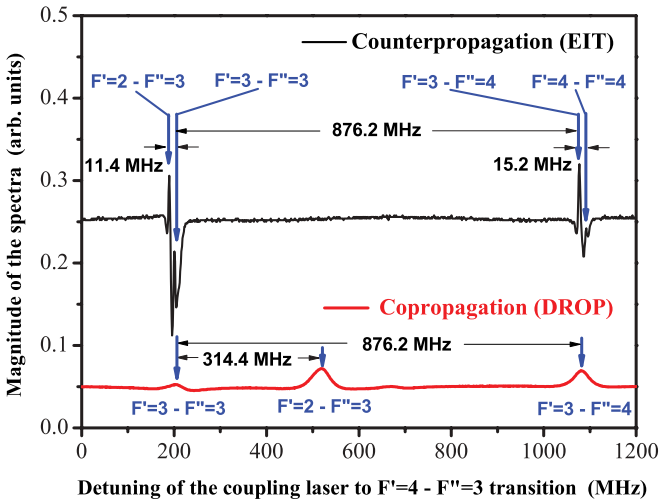

FIG. 5. (Color online) EIT spectra without Doppler background for counterpropagating (CTP) configuration and DROP spectra for copropagating (CT) configuration when the probe laser is locked to the $6S_{1/2}F = 3$–$6P_{3/2}F' = 3$ transition and the coupling laser is scanned over the $6P_{3/2}$–$8S_{1/2}$ transition.

effect (just considering stationary atoms $v = 0$), the calculated results show that there are no additional dips whether or not the wavelength of the probe laser is equal to that of the coupling laser. If the Doppler effect is taken into account, additional dips still do not exist when $\omega_p \approx \omega_c$, such as is the case for the rubidium $5S_{1/2}$–$5P_{3/2}$–$5D_{5/2}$ ladder-type system (corresponding transition wavelengths are 780.2 nm and 775.8 nm, respectively), which is a nearly perfect two-photon Doppler-free configuration for counterpropagating beams between the probe and coupling lasers. For us, based on the cesium $6S_{1/2}$–$6P_{3/2}$–$8S_{1/2}$ ladder-type system (corresponding transition wavelengths are 852.3 nm and 794.6 nm, $\omega_p \neq \omega_c$), additional dips are clearly shown in the calculated and experimental results. The stronger is the coupling laser, the deeper are the additional dips. In substance, these additional dips are from the term $-i(\omega_p - \omega_c)v/c$ for the residual Doppler effect due to the Doppler mismatch between the probe and the coupling lasers [18].

Furthermore, in theory, if we assume that the probe laser is locked to the $6S_{1/2}F = 3$–$6P_{3/2}F' = 3$ hyperfine transition and the coupling laser is scanned across the $6P_{3/2}$–$8S_{1/2}$ transition, the $6S_{1/2}F = 3$–$6P_{3/2}F' = 3$–$8S_{1/2}F'' = 3(4)$ system is the resonant EIT signal, and $6S_{1/2}F = 3$–$6P_{3/2}F' = 4$–$8S_{1/2}F'' = 3(4)$ and $6S_{1/2}F = 3$–$6P_{3/2}F' = 2$–$8S_{1/2}F'' = 3$ are regarded as detuning EIT signals, we can get a spectral structure similar to that shown in Fig. 4 with two peaks appended with 876.5-MHz frequency intervals from the $6P_{3/2}F' = 4$–$8S_{1/2}F'' = 3(4)$ hyperfine transitions due to transition selection rules, which are situated 14.6 MHz to the right of the $6P_{3/2}F' = 3$–$8S_{1/2}F'' = 3(4)$ peaks, respectively. This is expected in experiments, as shown in Fig. 5.

The $6P_{3/2}F' = 4$–$8S_{1/2}F'' = 3$ peak is too small to be seen in this EIT spectra. The frequency intervals for the two left peaks and the two right peaks are 11.4 and 15.2 MHz, respectively, which are close to the calculated values of 11.0 and 14.6 MHz. For DROP spectra, they have the same frequency intervals compared with Fig. 3. By comparing Figs. 3 and 5, we conclude that it is an advantage of using this EIT spectroscopic technique for measuring frequency intervals of hyperfine splitting in excited states, because the measured intervals are insensitive to frequency detuning of the probe beam. Any detuning of the probe laser would imply that it is resonant with nonzero certain velocity atoms. Ultimately, it only leads to the change of the relative magnitudes of these peaks and the whole shift of the EIT spectra while keeping unchanged frequency intervals.

IV. CONCLUSIONS

We experimentally demonstrate EIT signals without a Doppler background affecting the determination of the peak centers in a room-temperature atomic vapor cell. Experimental results are consistent with calculations based on a multilevel ladder-type model. The EIT spectra without a Doppler background and with a high SN ratio and a narrow line width undoubtedly will be helpful to precision measurement such as hyperfine splitting. In addition, we prove that another advantage of using this EIT spectroscopic technique for measuring hyperfine splitting is that the measured frequency intervals are insensitive to frequency detuning of the probe beam.

ACKNOWLEDGMENT

This work was partially supported by the National Natural Science Foundation of China (Grant No. 61078051, No. 60978017, No. 10974125, and No. 60821004), the NCET Program from the Education Ministry of China (Grant No. NCET-07-0524), and the Specialized Research Fund for the Doctoral Program of China (Grant No. 20070108003).

[1] A. Imamoglu and S. E. Harris, Opt. Lett. **14**, 1344 (1989).
[2] K. J. Boller, A. Imamoglu, and S. E. Harris, Phys. Rev. Lett. **66**, 2593 (1991).
[3] A. I. Lvovsky, B. C. Sanders, and W. Tittel, Nature Photon. **3**, 706 (2009).
[4] H. J. Briegel, W. Dur, J. I. Cirac, and P. Zoller, Phys. Rev. Lett. **81**, 5932 (1998).
[5] K. Banaszek, R. Demkowicz-Dobrzański, and I. A. Walmsley, Nature Photon. **3**, 673 (2009).
[6] J. M. Zhao, X. B. Zhu, L. J. Zhang, Z. G. Feng, C. Y. Li, and S. T. Jia, Opt. Express **17**, 15821 (2009).
[7] R. P. Abel, A. K. Mohapatra, M. G. Bason, J. D. Pritchard, K. J. Weatherill, U. Raitzsch, and C. S. Adams, Appl. Phys. Lett. **94**, 071107 (2009).
[8] H. X. Chen, A. V. Durrant, J. P. Marangos, and J. A. Vaccaro, Phys. Rev. A **58**, 1545 (1998).
[9] D. J. Fulton, S. Shepherd, R. R. Moseley, B. D. Sinclair, and M. H. Dunn, Phys. Rev. A **52**, 2302 (1995).
[10] L. Li and G. Huang, Phys. Rev. A **82**, 023809 (2010).
[11] J. Wang, L. B. Kong, X. Tu, K. J. Jiang, K. Li, H. W. Xiong, Y. F. Zhu, and M. S. Zhan, Phys. Lett. A **328**, 437 (2004).
[12] J. Gea-Banacloche, Y. Q. Li, S. Z. Jin, and M. Xiao, Phys. Rev. A **51**, 576 (1995).
[13] S. M. Iftiquar, G. R. Karve, and V. Natarajan, Phys. Rev. A **77**, 063807 (2008).
[14] Q. B. Liang, B. D. Yang, T. C. Zhang, and J. M. Wang, Opt. Express **18**, 13554 (2010).
[15] B. D. Yang, J. Y. Zhao, T. C. Zhang, and J. M. Wang, J. Phys. D: Appl. Phys. **42**, 085111 (2009).
[16] B. D. Yang, Q. B. Liang, J. He, T. C. Zhang, and J. M. Wang, Phys. Rev. A **81**, 043803 (2010).
[17] H. S. Moon, L. Lee, and J. B. Kim, J. Opt. Soc. Am. B **24**, 2157 (2007).
[18] A. K. Mohapatra, T. R. Jackson, and C. S. Adams, Phys. Rev. Lett. **98**, 113003 (2007).
[19] M. D. Lukin and A. Imamoglu, Phys. Rev. Lett. **84**, 1419 (2000).
[20] L. Deng, M. Kozuma, E. W. Hagley, and M. G. Payne, Phys. Rev. Lett. **88**, 143902 (2002).
[21] D. A. Steck, "Cesium D line data" (revision 2.1.4, 23 December 2010), [http://steck.us/alkalidata].